An experimental analysis of the flow through a driven mechanical model of the vocal folds

Bogdan R. Kucinschi [1], *Ronald C. Scherer* [2], *Kenneth J. DeWitt* [1,2], *Terry T. M. Ng* [1]

[1] Mechanical, Industrial and Manufacturing Engineering Department,
University of Toledo, Toledo, Ohio, USA
[2] Department of Communication Disorders,
Bowling Green State University, Bowling Green, Ohio, USA
bkucinsc@eng.utoledo.edu

Abstract

The production of voice is closely related to the flow of air through the glottis, whose shape is time-dependent. A number of experimental studies involving moving replicas of the vocal folds are available in the scientific literature, but they are generally restricted to one degree of freedom such that the glottal angles are fixed during the motion. In order to accurately reproduce the motion of the vocal folds, a scaled dynamically similar experimental apparatus that mimics the motion of the vocal folds using two degrees of freedom was built for the present study, such that both the glottal diameter and glottal angle change during a motion cycle. The motion of the model folds can be driven at different frequencies. The glottal flow is driven at a constant overall pressure, corresponding to the lung pressure. Both the transglottal pressure difference and flow rate were measured over the motion cycle, at different oscillation frequencies. Flow visualization was performed for a wide range of pressures and frequency. The results raise questions concerning the quasi-steady assumption.

1. Introduction

The production of voice, or phonation, is closely related to the oscillation of the vocal folds that induce fluctuations of the glottal air flow. The oscillation of the folds is a quasi-periodic process, whose characteristics (i.e., range of motion and frequency) depend on the interaction between fluid and structure. The oscillation frequency is around 110 Hz for males and 200 Hz for female speakers.

The relationship between the transglottal pressure drop and volumetric flow rate is important for the models used to predict the oscillation of the vocal folds. A large number of studies was dedicated to the investigation of the relationship between pressure and flow equations for situations relevant to speech production. The complexity of the motion of the vocal folds has deterred the use of moving experimental models. Static models were used instead, with shapes that correspond to different stages of oscillation of the folds (e.g., van den Berg et al., 1957, Scherer et al., 1983). Important pressure-flow equations were thus determined for a multitude of significant static cases. Most of the static studies were performed for symmetric glottal configurations, although asymmetric configurations were also investigated (Scherer et al., 2001).

There is a very limited amount of reported experimental work investigating the unsteady phenomena that occur during phonation. The work of Pelorson et al., 1995, investigates both experimentally and theoretically the unsteady flow through a few static models of the glottis, when the flow is driven by an abrupt pressure variation.

There are few studies reported that utilize dynamic vocal folds models. Deverge et al., 2003, reported a dynamic vocal fold model, which is composed of a set of rigid vocal folds replicas, one of which was given an oscillatory motion. A similar approach, this time using a set of elastic replicas, was reported by Zhang et al., 2002.

A simple mechanical model of the vocal folds was also reported by Barney et al., 1999. In this model a pair of shutters, driven by a vibration generator, mimic the vocal folds. The flow in the apparatus is provided by a constant flow rate source.

Prompted by the lack of a dynamic mechanical model that is able to realistically mimic the time-dependent glottal shape, a dynamic mechanical model was built. The motion of the vocal folds is approximated by a plan-parallel motion, composed of imposed translations and rotations. The generated motion is compatible with the first two eigenmodes of the vocal folds (Berry and Titze, 1996). The glottal angle can be controlled and synchronized with the glottal diameter. The flow is driven by a constant overall pressure, which mimics the lung pressure, which is reported to be relatively constant during phonation. The dynamic model allows for the measurement of the time-dependent flow rate and transglottal pressure for a range of overall (lung) pressures and driving frequencies.

The walls of the apparatus are transparent, such that flow visualizations inside the glottis can be performed. Flow visualizations are necessary to establish the character of the flow both inside and downstream of the glottis.

2. Experimental apparatus

A schematic of the experimental apparatus is shown in Fig.1. The replicas of the vocal fold surfaces were made of a deformable material (latex). Compared to the real-life dimensions, the model is scaled up by a factor of 7.5. As a consequence of the up-scaling of the model, dynamic similarity requires that the driving frequencies are decreased by the square of the scale factor. The motion of the vocal folds is driven by a computer-controlled mechanism. The driving mechanism is composed of two identical lever mechanisms,

each powered by a stepper motor (450SM-B3-HM, Aerotech Inc.). The motion of the two motors is coupled by software. Each lever mechanism drives a set of cylinders (see Fig.2), which helps shape the elastic material into a controlled configuration. Both the upper and lower sets are moved symmetrically with the centerline. A general view of the driving mechanism of the vocal folds is depicted in Fig.3. A top view close-up of the vocal folds is presented in Fig.4.

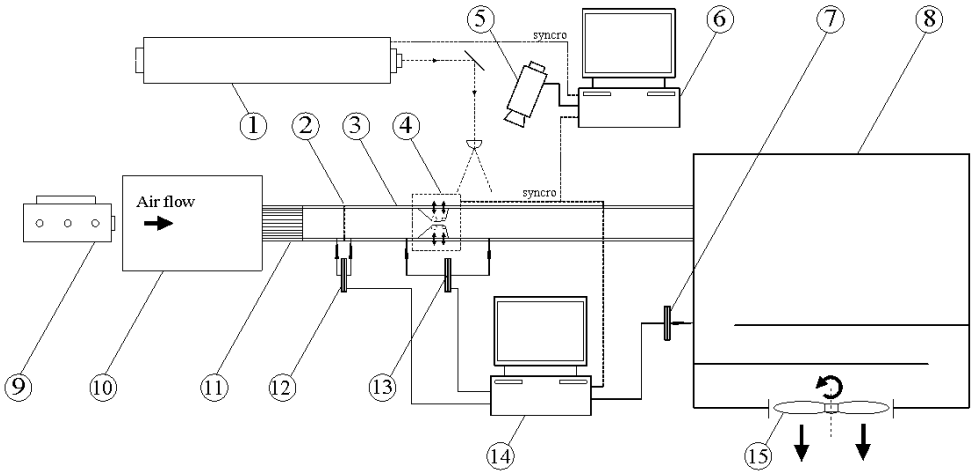

1. pulse laser
2. flowmeter net
3. plexiglass tunnel
4. dynamic vocal fold
5. digital camera
6. computer for flow visualization
7. pressure sensor for reservoir
8. constant pressure reservoir
9. smoke generator
10. entry reservoir
11. flow straightening section
12. pressure sensor for flow measurement
13. transglottal pressure sensor
14. computer for data acquisition
15. exhaust fan

Figure 1 *Schematic of the experimental device*

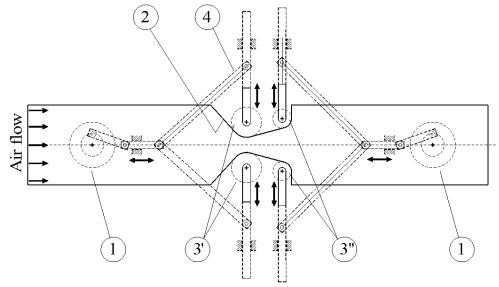

1 . stepper motors
2 . deformable material
3'. upstream cylinders
3". downstream cylinders
4 . levers

Figure.2 *Schematic of the driving mechanism*

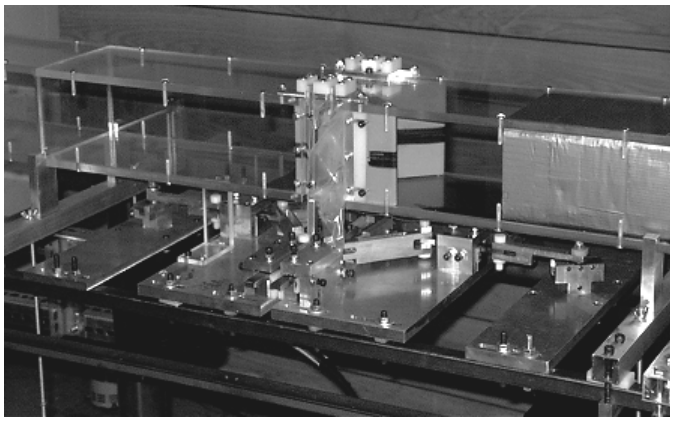

Figure 3 *General view of the driving mechanism of the vocal folds*

The total length of the experimental device mimics that of the human vocal tract, which allows for the presence of the inertance effects of the air in the sub- and supra-glottal segments in the vocal tract.

One can remark that the flow through the model is driven by a constant pressure source. The alternative constant flow rate condition is more convenient to impose, but it does not reflect physical reality.

In the model, the flow resistance of the glottis is much higher than the flow resistance anywhere else in the system.

A particularity of the apparatus is that the air is drawn by a lower pressure created downstream, as this was found more convenient from a constructive standpoint.

The variables of control are the amplitude of motion of the vocal folds (by setting up the amplitude of motion of the cylinders 3' and 3" in Fig.2), the phase between the upstream

and downstream margins of the vocal folds, the frequency of oscillation, and the overall driving pressure (corresponding to lung pressure).

The experiments were performed for a set of three lung pressures, i.e., 4, 8 and 12 cmH_2O real-life. As the model is 7.5 times larger than real-life, the corresponding pressures in the model are smaller by a factor of 7.5^2 than the real-life ones. Thus, the driving pressures used in the model were 7, 14 and 21 Pa. The measurement of such small pressures necessitates the use of extremely accurate pressure sensors (Valedyne DP103 series, Valedyne Engineering) for the transglottal pressure difference.

The dynamic similarity requires that the model frequency be equal to the real-life frequency divided by the square of the scale factor. The frequencies used for the experimental tests were 0.5, 1, 1.5, 2 and 2.5 Hz, corresponding to real-life frequencies of 28.1, 56.2, 84.4, 112.5 and 140.6 Hz. Also, tests were performed for static configurations in the cycle of glottal motion.

The volume flow rate was measured via a custom-made pneumotach. Thus, the pressure drop over a metallic net, 2 (see Fig.1) was measured by a pressure sensor. The flow resistance of the metallic net was extremely low, about one order of magnitude less than that of the vocal folds.

As the DP103 pressure sensors have a poor frequency response even at low frequency, special corrections for amplitude and phase were used in order to obtain reliable results. The corrections required the construction of a separate experimental rig that permitted the comparison of the output signal of the sensor with a reference variable pressure of known amplitude and frequency.

Flow visualization with glycol-based smoke was performed by using a second acquisition system. Two laser sheets were shed from both upstream and downstream of the folds, such that the glottal region can be observed regardless of the glottal angle. Any glottal position can be investigated by synchronizing the pulse of the laser by means of a position signal provided by the apparatus.

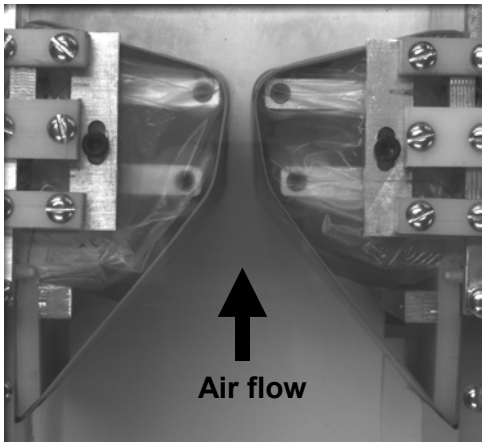

Figure 4 *Top view of the dynamic vocal folds*

The mechanism was set such that the motion of the downstream set of deformers lags the upstream set by 90°. The beginning of a cycle corresponds to the upstream set of deformers being in the closest position (i.e., smallest glottal gap). Figure 5 presents certain positions of the vocal folds vs. the driving angle, θ, which is the angle of rotation of the motor driving the upstream set of deforming cylinders. The glottal diameters (in cm real-life) and glottal angles are presented in Table 1 for certain positions. The positive glottal angles correspond to the divergent shapes, while the negative ones represent convergent shapes.

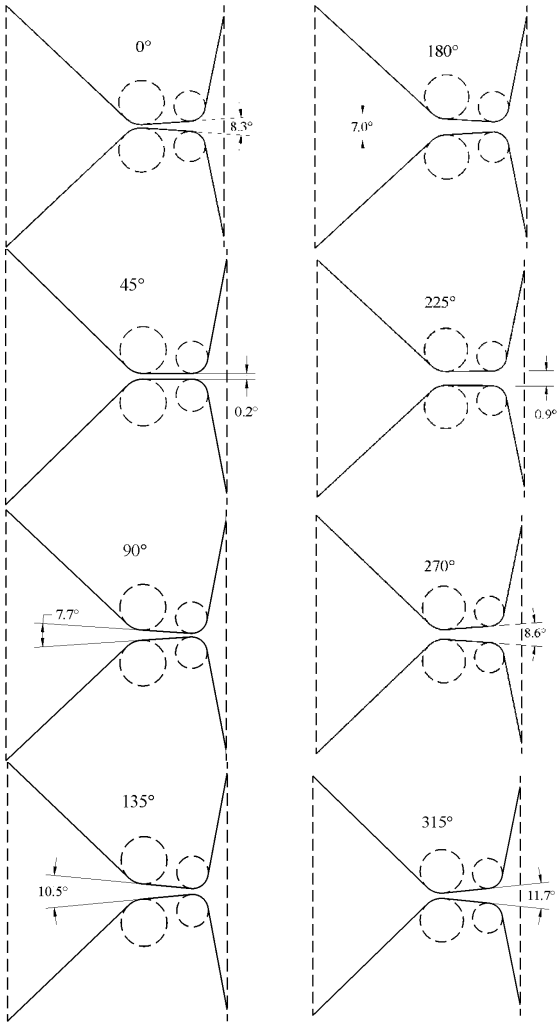

Figure 5 *Glottal shape for certain values of θ*

Table 1: *Glottal parameters for certain values of θ*

Driving angle, θ [°]	Glottal diameter, D_g [cm]	Glottal angle, α_g [°]
0	0.025	+8.3
90	0.025	-7.7
180	0.075	-7.0
270	0.072	+8.6

3. Results of flow and pressure measurements

Flow rates and transglottal pressures were measured over a complete vocal fold motion cycle, both for the static case and for dynamic cases at different frequencies. In the first case, the measurements were performed for static configurations corresponding to fixed driving angles θ. The values of θ cover the complete motion cycle, i.e., from 0 to 360°.

As the glottal diameter and the glottal angle are coupled through the geometry of the mechanism, their variation depends on the configuration of the apparatus. Thus, for θ from 0 to 90°, the glottal diameter, D_g, is roughly constant (around 0.025 cm real-life), while the glottal angle is changing from 8.3° divergent to 7.7° convergent. One can observe that the flow rate decreases with θ in the 0-90° range, regardless of the frequency of the folds and of the overall pressure (see Figs.6-8). It appears that, when the lung pressure is constant, the smallest value of the flow rate occurs for the highest convergent angle and smallest glottal diameter.

For driving angles θ in the 90-180° range, the folds remain convergent (changing slightly from 7° to 10.5°), while the glottal diameter increases almost linearly. The tendency of the flow rate is to increase with the glottal diameter. For driving angles θ in the 180-270° range, the glottal angle changes from a convergent (7°) to a divergent position (8.6°), while the glottal diameter stays around a maximal value (0.075 cm real-life). Thus, a divergent glottal angle produces a larger flow rate for the same diameter, consistent with the same trend observed for θ in the 0-90° range.

For driving angles θ between 270 and 360°, the glottis stays divergent (the glottal angle fluctuating slightly in the range 8.2-11.7°), while the glottal diameter returns to the minimal value of 0.025 cm real-life. As expected, the flow rate decreases on this portion of the cycle.

The trends of the transglottal pressure difference (see Figs.9-11) are generally quite the opposite of those observed for the flow rate. Also, the trends described above are valid for the static case as well as for the situations where the folds are driven at various frequencies.

The figures show that the peak-to-peak flow rate and transglottal pressure drop amplitudes decrease as the frequency increases. Also, the location of the minimum and maximum flow rates is delayed more (i.e., shifted to the right) with the increase of frequency. As well as the flow rate, the transglottal pressure difference depends on the motion of the vocal folds. Figures 9 to 11 show that the amplitude of the pressure change depends upon frequency. The amplitude decrease for both flow rate and transglottal pressure, as well as the delay, are due to the inertance of air in the vocal tract. The inertive pressure downstream the folds is proportional to the time derivative of the flow rate.

It is of interest to observe that the flow rates depend almost linearly on the lung pressure, at any driving angle θ. It can be seen in Figs.12 and 13 that the inlet flow rates for 8 cmH_2O are almost at the middle between the curves corresponding to lung pressures of 4 and 12 cmH_2O (for the static case and for 112 Hz, respectively).

The flow resistance for the static case is shown in Fig.14, expressed in $M\Omega_a$, Ω_a =kg $m^{-4}s^{-1}$. The resistance depends on the glottal diameter and glottal angle particular for each angle θ. Larger resistances are associated with smaller glottal diameters. Also, convergent glottal angles seem to lead to larger resistances than divergent angles, and the resistances are generally larger for higher lung pressures.

Glottal flow resistance, defined as the ratio of the transglottal pressure to the mean flow rate through the glottis, is represented in Fig.15 for certain frequencies, for a lung pressure of 8 cmH_2O. An interesting behavior of the flow resistance can be observed for the first part of the glottal cycle (i.e., up to angles θ of around 180°). Here, the measured resistance for the static case is larger than that corresponding to the dynamic cases. On the contrary, there are relatively smaller differences between the resistance curves for the second part of the cycle. Although only the 8 cmH_2O case is represented here, similar trends were observed for lung pressures of 4 and 12 cmH_2O.

The first part of the cycle is characterized by an increasing diameter of the folds, when the glottal volume increases, while in the second part of the cycle the folds close and the glottal volume decreases. It seems that in the first phase of the cycle, when the glottal angle is mainly convergent and the glottal diameter increases almost linearly, the dynamic effects are not negligible, as suggested by the quasi-steady assumption.

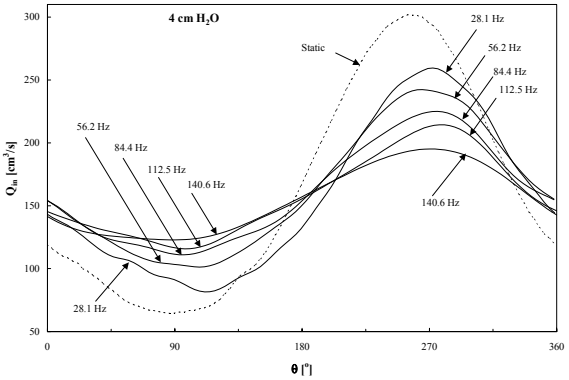

Figure 6 *Inlet flow rate over a cycle, 4 cmH_2O*

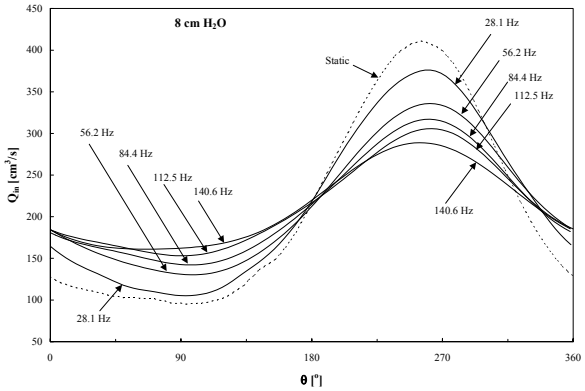

Figure 7 *Inlet flow rate over a cycle, 8 cmH_2O*

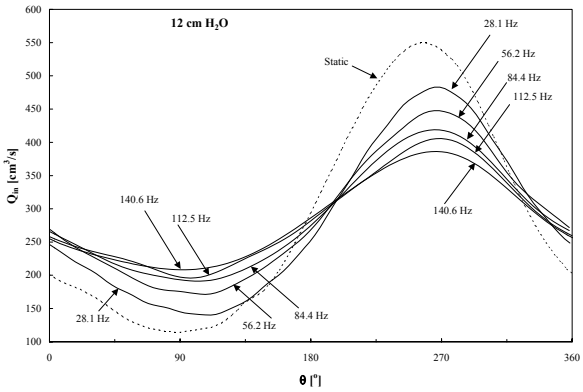

Figure 8 *Inlet flow rate over a cycle, 12 cmH_2O*

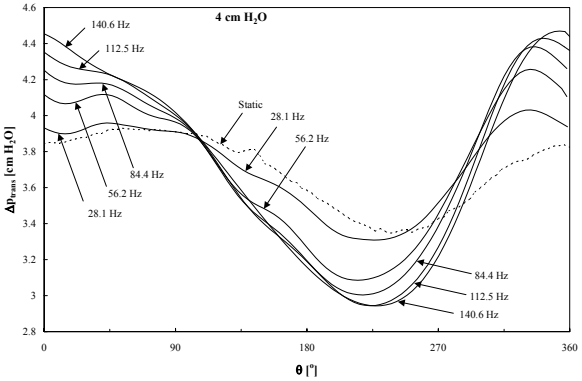

Figure 9 *Transglottal pressure drop over a cycle, 4 cmH_2O*

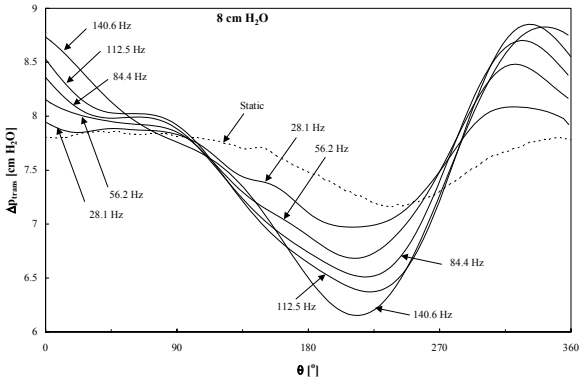

Figure 10 *Transglottal pressure drop over a cycle, 8 cmH_2O*

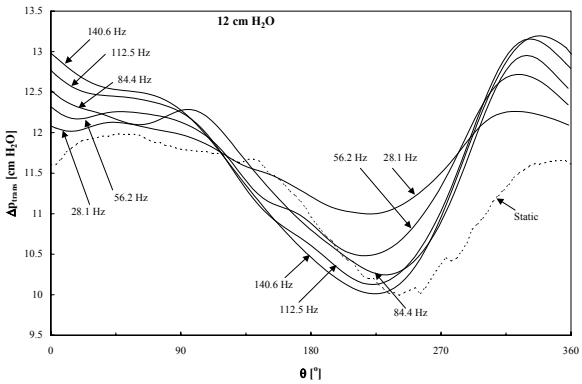

Figure 11 *Transglottal pressure drop aver a cycle, 12 cmH_2O*

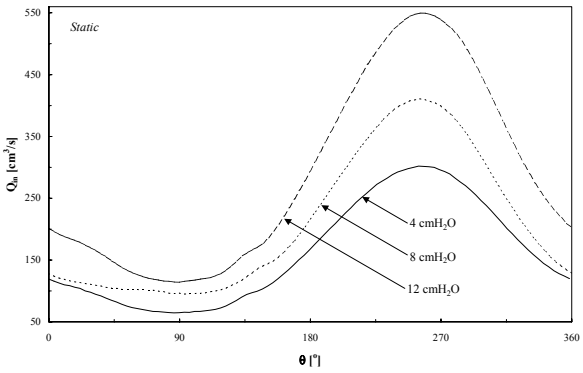

Figure12 *Flow rate for different lung pressures, static case*

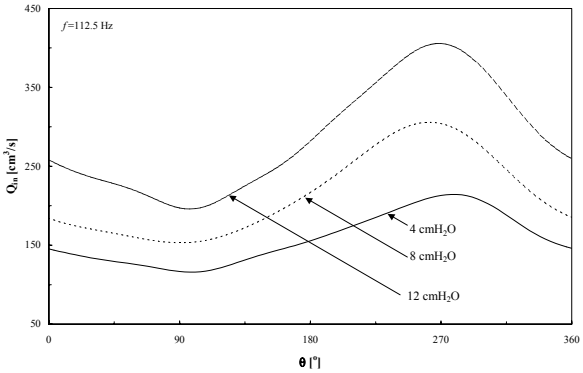

Figure13 *Flow rate for different lung pressures, f =112.5 Hz*

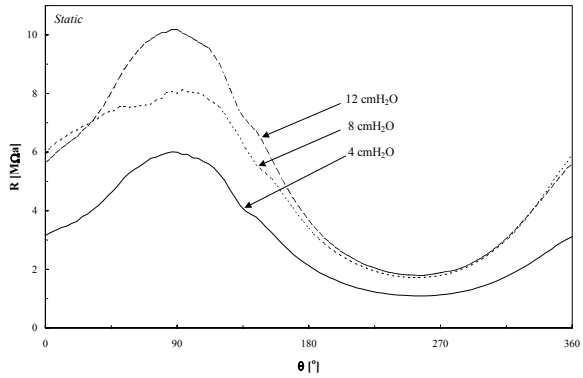

Figure 14 *Flow resistance for different pressures, static case*

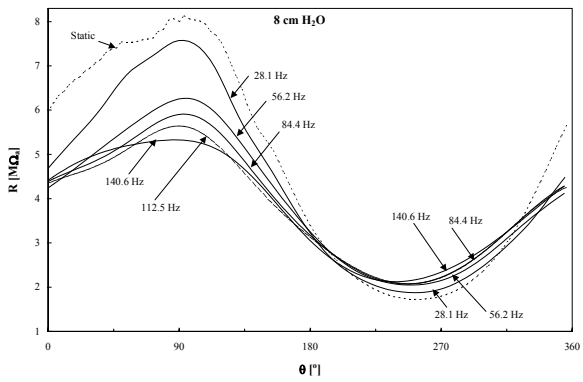

Figure 15 *Flow resistance over a cycle, 8 cmH_2O*

4. Flow visualizations

The flow visualization was performed for lung pressures of 4, 8 and 12 cmH_2O, in the static case as well as for frequencies in the range 28.1-140.6 Hz. A number of four positions were initially investigated (i.e., $\theta = 0°$, 90°, 180° and 270°).

For the position 90°, for which the glottal angle is convergent and the glottal diameter is small (see Table 1), a laminar jet was observed, both for static and dynamic cases (see Fig.16). The jet separates slightly upstream from the exit, due to the diverging nature of the exit curvature. The jet remains laminar for a distance until transition occurs. This distance generally increases with the frequency of oscillation. Eventually Kelvin-Helmholtz instability vortices occur, followed by turbulent dissipation. The jet symmetry is more evident in the dynamic cases than for the static situation.

For the position 180°, for which the glottal angle is convergent and the glottal diameter is large, all of the emerging jets are laminar and symmetric (see Fig.17). All transition locations occur outside of the glottis. The separation points on the glottal walls move downstream toward the glottal exit with increasing pressure and increasing frequency.

The position 270° is characterized by a divergent glottal angle and a large glottal diameter (similar to that for the 180° position). The emerging jets are laminar and symmetric for all pressure and frequency cases, and the transition locations occur outside of the glottis (see Fig.18). The separation points on the glottal walls are the same for all pressures and increase downstream with frequency.

The most intriguing position is that for 0°. This position is divergent and has a small glottal diameter. At this position a laminar jet emerges from the glottis and presents a transition point outside the glottis only for the static case and the lowest frequency, 28.1 Hz. For all the other dynamic cases, the transition occurs inside the glottis. The glottal jets are not symmetric and are bi-stable in direction for all cases. Figure 19 presents a visualization for 140.6 Hz and a lung pressure of 8 cmH_2O. One can observe the presence of Kelvin-Helmholtz instability vortices, and transition occurs axially around the middle of the glottis. For higher lung pressures there are cases where the jet becomes fully turbulent while inside the glottis.

Further static and dynamic experiments were conducted in a range for a driving angle θ of -50° to +10°, where the glottal angle is divergent and the glottal diameter decreases. As Fig.5 shows, the glottal volume decreases for θ from 270° to 0°. The flow visualization results also show that there are cases in this range when the glottal vortices may occur even for particular static configurations. The corresponding pictures are not shown here in order to keep this material within a reasonable length.

Vortex shedding close to solid boundaries can provide a secondary source of acoustic energy. Recently, Barney et al., 1999, performed an experimental investigation of a shutter-type dynamic mechanical model and showed that the vortices in the shutter area provide significant acoustic sources.

The flow visualization results show that, for the case of moving vocal folds, the glottal flow is very complex and may be laminar, transitional and turbulent, depending on the pressure forcing function, frequency, and glottal diameter and angle. This appears to question the assumption of quasi-steadiness of the flow, since the character of the glottal flow may be totally different between a moving case and the corresponding static situation.

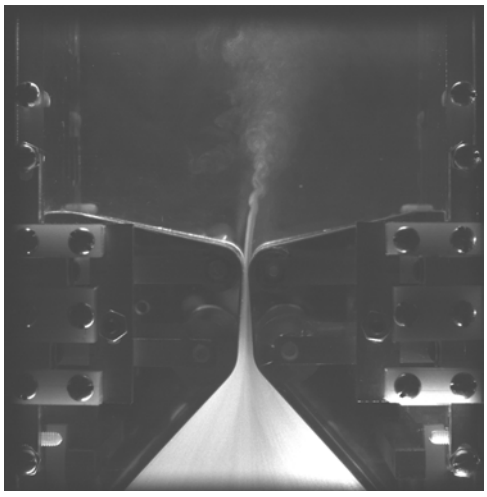

Figure 16 *Glottal flow, position 90°, 4 cmH_2O, 140.6 Hz*

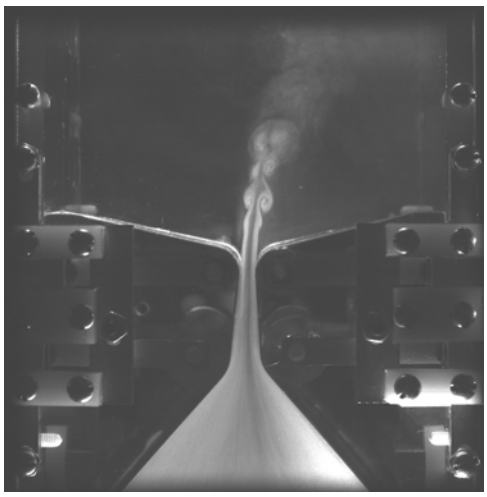

Figure 17 *Glottal flow, position 180°, 4 cmH_2O, 84.4 Hz*

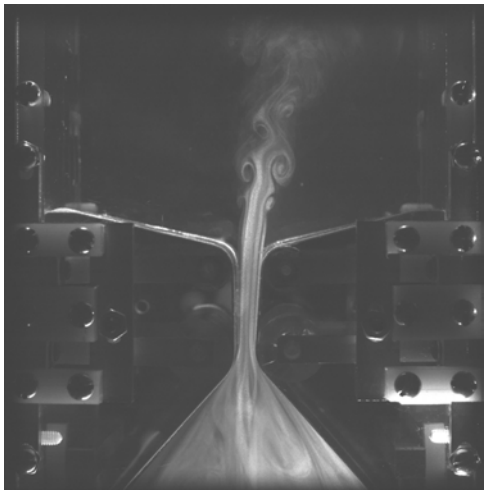

Figure 18 *Glottal flow, position 270°, 4 cmH_2O, 112.5 Hz*

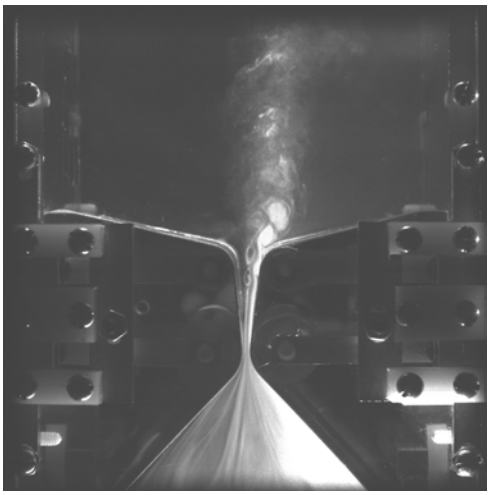

Figure 19 *Glottal flow, position 0°, 8 cmH_2O, 140.6 Hz*

5. Conclusions

The purpose of the present research was to investigate the relationship between the flow rate and transglottal pressure difference for the moving vocal folds, as well as to determine the flow patterns inside and downstream of the glottis in connection to the frequency of the movement of the folds. It was also sought to answer, at least in the framework of the present experimental conditions, the question if the quasi-steady assumption is valid in the study speech production.

The measurements show that both the flow rate and transglottal pressure are affected by the frequency of the vocal folds. The inertance of air in the trachea and vocal tract, together with the unsteady flow rate produces a fluctuation of pressure both downstream and upstream of the glottis, which is reflected in a frequency-dependent transglottal pressure drop.

It was observed that for the present experimental configuration, the measured flow rates are lower for the convergent than for divergent glottal angles for roughly the same glottal diameter. As expected, the flow rate also increased with the glottal diameter when the glottal angle was kept roughly constant.

The glottal flow resistance was calculated as the ratio of the measured transglottal pressure difference and the flow rate. Since in the moving case the inlet flow rate is not equal to the outlet flow rate, the average of the inlet and outlet flow rates was used to determine the flow resistance. It appears that, in the part of the glottal cycle that corresponds to the closing phase of the folds (i.e., when the glottal volume decreases), the values of the static resistance are similar to the resistance obtained for moving folds. However, this is not valid in the parts of the cycle where the glottal volume increases. This questions the validity of the quasi-steady assumption. Other geometric cases will be studied, such that a set of conditions for which the dynamic effects are important may be found.

The flow visualization technique was used to examine the character of the flow inside and downstream of the glottal area. It was observed that the flow can be laminar, transitional and turbulent, depending not only on the shape of the glottis and lung pressure, but also on the frequency of motion of the vocal folds. Thus, the quasi-steady assumption, which states that the flow behaves at any frequency the same as in the static situation, appears to be questionable. The flow visualization revealed, for certain experimental conditions, the presence of Kelvin-Helmholtz vortices inside the glottis, which may constitute an additional source of acoustic energy.

Acknowledgement
This research was support by NIH grant # 2 R01 DC03577.

6. References

[1] Barney, A., Shadle, C.H., Davies, P.O., 1999. Fluid flow in a dynamic mechanical model of the vocal folds and tract. I. Measurements and theory. *J.Acoust.Soc.Am.*, 105(1), 444-455.

[2] Berry, D.A., Titze, I.R., 1996. Normal modes in a continuum model of vocal fold tissues. *J.Acoust.Soc.Am*. 100(5), 3345-3354.

[3] Deverge, M., Pelorson, X., Vilain, C., Lagrée, P.Y., Chentouf, F., Willems, J., Hirschberg, A., 2003. Influence of collision on the flow through in-vitro rigid models of the vocal folds. *J.Acoust.Soc.Am*. 114(6), 3354-3362.

[4] Pelorson, X., Hirschberg, A., Wijnands, A.P., Baillet, H., 1995. Description of the flow through in-vitro models of the glottis during phonation. *Acta Acustica*. 3, 191-202.

[5] Scherer, R. C., Titze, I. R., Curtis, J. F., 1983. Pressure-flow relation-ships in two models of the larynx having rectangular glottal shapes. *J.Acoust.Soc.Am*. 73(2), 668-676.

[6] Scherer, R.C., Shinwari, D., DeWitt, K., Zhang, C., Kucinschi, B., Afjeh, A., 2001. Intraglottal pressure profiles for a symmetric and oblique glottis with a divergence angle of 10 degrees. *J.Acoust.Soc.Am*. 109 (4), 1616-1630.

[7] van den Berg, J.W., Zantema, J.T., Doornenball, P., 1957. On the air resistance and the Bernoulli effect of the Human Larynx. *J.Acoust.Soc.Am*. 29, 626-631.

[8] Zhang, Z., Mongeau, L., Frankel, S.H., 2002. Experimental verification of the quasi-steady approximation for aerodynamic sound generation by pulsating jets in tubes. *J.Acoust.Soc.Am*. 112(4), 1652-1663.